Energy band alignment at Cu_2O/ZnO heterojunctions characterized by *in situ* x-ray photoelectron spectroscopy*

Yan Zhao(赵妍), Hong-Bu Yin(尹泓卜), Ya-Jun Fu(符亚军), Xue-Min Wang(王雪敏), and Wei-Dong Wu(吴卫东)†

Science and Technology on Plasma Physics Laboratory, Research Center of Laser Fusion, China Academy of Engineering Physics, Mianyang 621900, *China*

(Received 25 November 2018; revised manuscript received 6 May 2019; published online 9 July 2019)

With the increasing interest in Cu_2O-based devices for photovoltaic applications, the energy band alignment at the Cu_2O/ZnO heterojunction has received more and more attention. In this work, a high-quality Cu_2O/ZnO heterojunction is fabricated on a *c*-Al_2O_3 substrate by laser-molecular beam epitaxy, and the energy band alignment is determined by x-ray photoelectron spectroscopy. The valence band of ZnO is found to be 1.97 eV below that of Cu_2O. A type-II band alignment exists at the Cu_2O/ZnO heterojunction with a resulting conduction band offset of 0.77 eV, which is especially favorable for enhancing the efficiency of Cu_2O/ZnO solar cells.

Keywords: Cu_2O, ZnO, x-ray photoelectron spectroscopy, laser-molecular beam epitaxy

PACS: 73.40.Lq, 82.80.Pv, 77.55.hf, 73.20.At **DOI:** 10.1088/1674-1056/28/8/087301

1. Introduction

With the urgency of both the energy crisis and the aggravation of environmental pollution, the search for an alternative fuel source that is clean, environmental-friendly and reproducible has received increasing attention. As the cleanest energy, solar cells are a renewable energy that is being developed as an alternative source to traditional fossil fuel-based sources. During the last ten years, the most successful oxide solar cells were based on heterostructures of Cu_2O. In 2011, interest was renewed due to the conversion efficiency increasing up to 3.8% of Cu_2O/ZnO solar cells in the material for photovoltaic applications.[1,2] Cu_2O is a promising p-type semiconductor with a direct band gap (E_g) of 2.17 eV. Its common p-type conductivity is due to copper vacancies with an ionization energy of 0.28 eV.[3] Zinc oxide (ZnO) is an intrinsically doped n-type semiconductor with a direct band gap of 3.37 eV.[4] In the past years, the conversion efficiency of Cu_2O/ZnO-based cells has been improved significantly. So far, the highest achieved conversion efficiency of Cu_2O/ZnO-based cells is only 4.13%,[5] even though an upper limit of 18% is theoretically predicted.[6] Generally, the efficiency enhancement is associated with the suppression of the recombination current, which is due to a large conduction band discontinuity at the interface.[7] In the case of the Cu_2O/ZnO heterojunction, the small conduction band offset (CBO), which is required by high-efficiency solar cells, has been a research focus.[8] Several groups have reported on regulating the band alignment of Cu_2O/ZnO interfaces.[9–11] However, defects leading to a considerable modification of energy band alignment are often formed during the fabrication of the interface. This is especially true for the Cu_2O/ZnO heterointerface, where the presence of metallic Zn, metallic Cu or CuO can lead to a modification of the energy band alignment. Several methods have been employed for fabricating Cu_2O/ZnO heterointerfaces, including the electrochemical deposition method,[12,13] radio-frequency magnetron sputtering,[14] an ion beam sputtering method,[15] and low-damage deposition methods.[16,17] But up to now, few studies have focused on the fabrication of a Cu_2O/ZnO heterojunction with laser-molecular beam epitaxy (L-MBE). In this study, we report on the growth of Cu_2O/ZnO heterojunction by L-MBE. The energy band alignment of the Cu_2O/ZnO heterojunction is systematically investigated by *in situ* x-ray photoelectron spectroscopy.

2. Experiment

Cu_2O/ZnO films were grown on *c*-Al_2O_3 substrates using L-MBE. Sintered ZnO (purity, 99.9995%) and CuO (purity, 99.9%) ceramic targets were ablated by a KrF excimer laser (248 nm, 350 mJ, 1 Hz, and 25 ns). The substrates were mounted 5 cm away from the target in an ultra-high vacuum chamber with a base pressure prior to 2×10^{-7} Pa. The investigation of the energy band alignment was carried out using *in situ* x-ray photoelectron spectroscopy (XPS). The XPS spectra were performed in an ultra-high vacuum chamber (5×10^{-8} Pa) equipped with an unmonochromatized Al Kα source (1486.6 eV). The layer thickness was precisely controlled by the product of the deposition time and deposition rate, which were predetermined by single-layer deposition ex-

*Project supported by the National Natural Science Foundation of China (Grant No. 11404302) and the Laser Fusion Research Center Funds for Young Talents, China (Grant No. RCFPD1-2017-9).

†Corresponding author. E-mail: wuweidongding@163.com

© 2019 Chinese Physical Society and IOP Publishing Ltd

periments.

In this study, three sets of samples were prepared in order to clarify the electronic band configuration of the Cu_2O/ZnO heterojunction: (i) 100-nm-thick ZnO film grown on a c-Al_2O_3 substrate to measure the valence band maximum (VBM) and Zn 2p core level (CL), named the ZnO sample; (ii) 100-nm-thick Cu_2O/100-nm-thick ZnO films grown on a c-Al_2O_3 substrate to measure the VBM and Cu 2p CL, called the Cu_2O sample; (iii) 10 nm-thick Cu_2O/100-nm-thick ZnO films grown on a c-Al_2O_3 substrate to determine the difference in the CLs of Cu 2p and Zn 2p, referred to as the Cu_2O/ZnO heterojunction sample. The x-rays could go through the 10-nm-thin Cu_2O film but could not pass through the 10-nm-thick Cu_2O film. The XPS spectra were accurately calibrated by the C 1s peak (284.6 eV) to compensate for the charge effect, and the total energy resolution of this XPS system was less than 0.05 eV, which usually affects the measured kinetic energy of photoelectrons.[18]

Kraut's method is a direct and useful tool to determine the valence band offsets (VBOs), and has been used to measure the valence band discontinuities of heterojunctions.[19–21] This CL photoemission-based method was employed for semiconductor/semiconductor heterojunctions.[22] However, due to the insulating properties of dielectrics, neutralization differential charging and Fermi edge decoupling effects were not negligible for heterostructures with dielectrics.[23,24] Based on Kraut's method, the VBO of the Cu_2O/ZnO interface can be described by the following formula[22]

$$\Delta Ev = \Delta E_{\mathrm{CL}} + (E^{\mathrm{Cu_2O}}_{\mathrm{Cu2p}} - E^{\mathrm{Cu_2O}}_{\mathrm{VBM}}) - (E^{\mathrm{ZnO}}_{\mathrm{Zn2p}} - E^{\mathrm{ZnO}}_{\mathrm{VBM}}), \quad (1)$$

where

$$\Delta E_{\mathrm{CL}} = E^{\mathrm{Cu_2O/ZnO}}_{\mathrm{Zn2p}} - E^{\mathrm{Cu_2O/ZnO}}_{\mathrm{Cu2p}} \quad (2)$$

is the energy difference between Zn 2p and Cu 2p, which are measured in the heterojunction sample; $E^{\mathrm{Cu_2O}}_{\mathrm{Cu2p}}$ and $E^{\mathrm{Cu_2O}}_{\mathrm{VBM}}$ are the values of the CL energy and VBM from the Cu_2O sample; $E^{\mathrm{ZnO}}_{\mathrm{Zn2p}}$ and $E^{\mathrm{ZnO}}_{\mathrm{VBM}}$ are the values of the CL energy and VBM from the ZnO sample, respectively.

3. Results and discussion

To investigate the interface of the heterostructure sample, a cross-sectional scanning electron microscope (SEM) image and energy dispersive spectrometer (EDS) analysis were obtained and are displayed in Fig. 1. It is obvious that the ZnO film has been grown on a c-Al_2O_3 substrate, followed by Cu_2O film deposition. The element analysis of the region marked by the white rectangle in the SEM image is carried out by EDS, and shown in Figs. 1(c)–1(e). Figure 1(b) displays the Cu_2O/ZnO interface region observed in a high-resolution transmission electron microscope (HRTEM). Although the interface between Cu_2O and ZnO is not very clear, two different compounds are clearly distinguished by the red dashed line. The Cu_2O crystallizes into a cubic structure with parameter $a_{Cu_2O} = 0.427$ nm, while the interplanar distance is 0.30 nm corresponding to the distance between the two adjacent Cu_2O (110) crystal planes. The interplanar distance is 0.26 nm corresponding to the distance between the two adjacent (0 0 0 2) crystal planes of ZnO with hexagonal wurtzite structure.

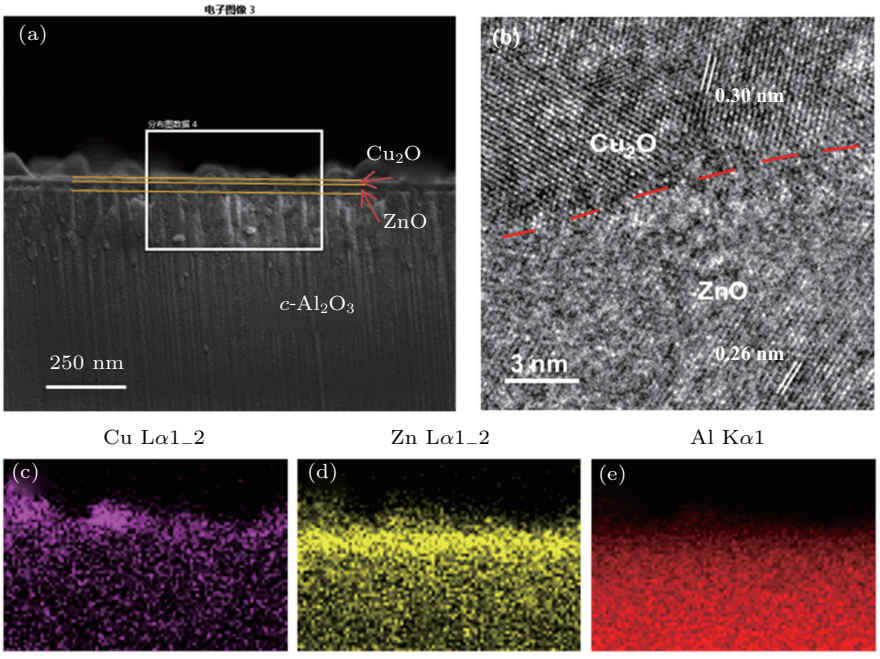


Fig. 1. (a) Cross-section SEM image, (b) HRTEM of Cu_2O/ZnO interface, (c)–(e) cross-section element mapping by EDS of Cu_2O/ZnO heterojunction sample.

Figure 2 shows the XRD θ–2θ scan pattern of 100 nm-Cu_2O/100 nm-ZnO/c-Al_2O_3 grown on a c-Al_2O_3 substrate. Besides the c-plane Al_2O_3 substrate diffraction peak at 41.71°, only the pronounced (0 0 0 2) and a (0 0 0 4) peak of ZnO in the XRD pattern are observable at 34.35° and 72.30°, which shows that the ZnO film is of hexagonal wurtzite structure, and highly c-axis oriented without any impurity phases. The peak at 61.23° can be assigned to Cu_2O (220), which reveals a preferred orientation of (110) for Cu_2O. Therefore, it can be concluded that the Cu_2O/ZnO heterojunction is grown on a c-Al_2O_3 substrate with the orientation relationship of $Cu_2O(110)\|ZnO\ (0002)\|Al_2O_3\ (0001)$.

All the core-level peaks are fitted using a Shirley background and Voigt (mixed Lorentzian–Gaussian) line shapes. The binding energy for each of the CL peaks is precisely taken as the energy corresponding to the maximum intensity. Figure 3(a) shows the XPS survey scan of the Zn $2p_{3/2}$ CL of the ZnO sample, while the peaks located at 1021.35 eV and 1044.13 eV are assigned to the electronic states of Zn $2p_{3/2}$ and Zn $2p_{1/2}$, respectively. The Zn element exists only in the oxidized state, which confirms that no evidence of the metallic Zn peak is observed. In addition, the peak of Zn $2p_{3/2}$ CL has a symmetric shape, implying a uniform Zn–O bonding state. The valence band spectrum of 100 nm-ZnO/c-Al_2O_3 is shown in Fig. 3(b) and is used to measure the VBM position. The VBM position with respect to the surface Fermi level is obtained by the intersection of linear fits to the leading edge of the valence band photoemission and the ground.[25–27] This linear method has already been widely used to determine the VBM of semiconductors with an accuracy of about ±0.05 eV.[28,29] Focusing on the inset of Fig. 3(b), it is worth noting that the peak at ∼ 0 eV in the inset is a distinct satellite feature induced by Al Kα, which is marked by the red solid square. The VBM value of the ZnO sample relative to E_F is determined to be 2.44 ± 0.05 eV.

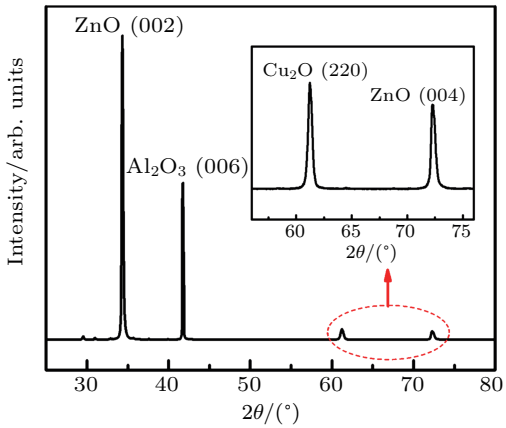


Fig. 2. XRD θ–2θ scan patterns of 100-nm-Cu_2O/100 nm-ZnO/c-Al_2O_3.

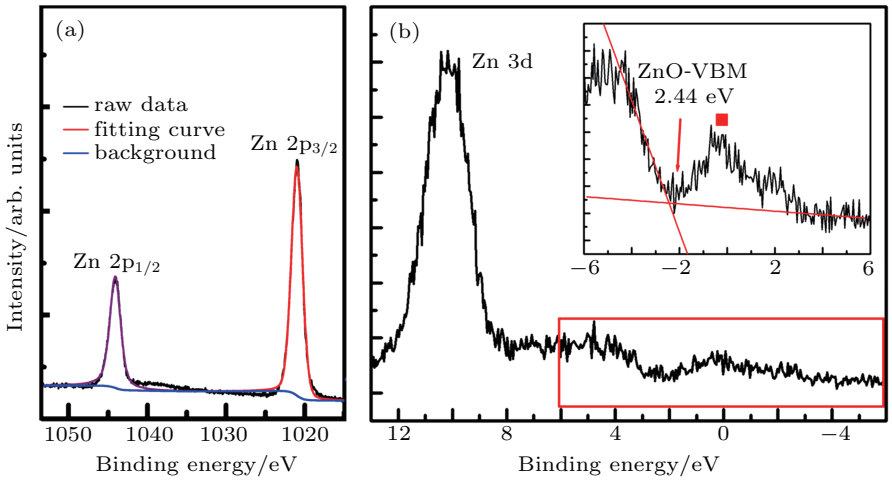


Fig. 3. XPS survey scan of 100 nm-ZnO/c-Al_2O_3 (a) Zn $2p_{3/2}$ CL spectrum; (b) valence band spectrum, with inset showing VBM determination.

The XPS scan spectrum of 100 nm-Cu_2O/100 nm-ZnO/c-Al_2O_3 is shown in Fig. 4(a). The Cu $2p_{3/2}$ and $2p_{1/2}$ peak are observed at 932.4 eV and 952.3 eV, respectively. To identify the chemical state of the Cu element in the Cu_2O sample, XPS and x-ray-excited Auger spectra (XAES) are measured. The absence of characteristic shakeup satellites of CuO located at ∼ 9 eV, which is higher than the binding energy of the main $2p_{3/2}$ and $2p_{1/2}$ peak, indicates that the Cu species should not be Cu^{2+}.[30] Then, Cu^0 and Cu^{1+} could be easily distinguished from the XAES of Cu L_3VV. The characteristic kinetic energy values of the different oxidation states of Cu are shown in Ref. [30]. The major Cu LVV Auger peak with kinetic energy of 916.3 eV is presented in Fig. 4(b), which is attributed to Cu^{1+}. It has been reported that the Cu Auger spectrum has a distinct satellite feature at a kinetic energy of ∼ 2.5 eV higher than the main peak.[30–32] The absence of the satellite peak of Cu in the presented curves also implies that the Auger peaks are associated with Cu^{1+}, which is consistent with the XRD result in Fig. 2. Besides, this conclusion is further supported by the appearance of a weak peak at around 965 eV (marked

by a red rectangle in Fig. 4(a)), which is in good agreement with the satellite peak position of Cu_2O.[31] Like the ZnO sample, the VBM value of the Cu_2O sample relative to E_F is determined to be 0.14 ± 0.05 eV, which is illustrated by Figs. 4(c) and 4(d).

Figures 5(a) and 5(b) show the Zn $2p_{3/2}$ CL spectrum and Cu $2p_{3/2}$ CL spectrum of 10 nm-Cu_2O/100 nm-ZnO/c-Al_2O_3. The peak of the Zn $2p_{3/2}$ CL of the Cu_2O/ZnO heterojunction located at 1021.00 eV is shifted by 0.35 eV compared with that of the ZnO sample. Correspondingly, the Cu $2p_{3/2}$ peak located at 932.19 eV is shifted by 0.02 eV compared with that of the Cu_2O sample.

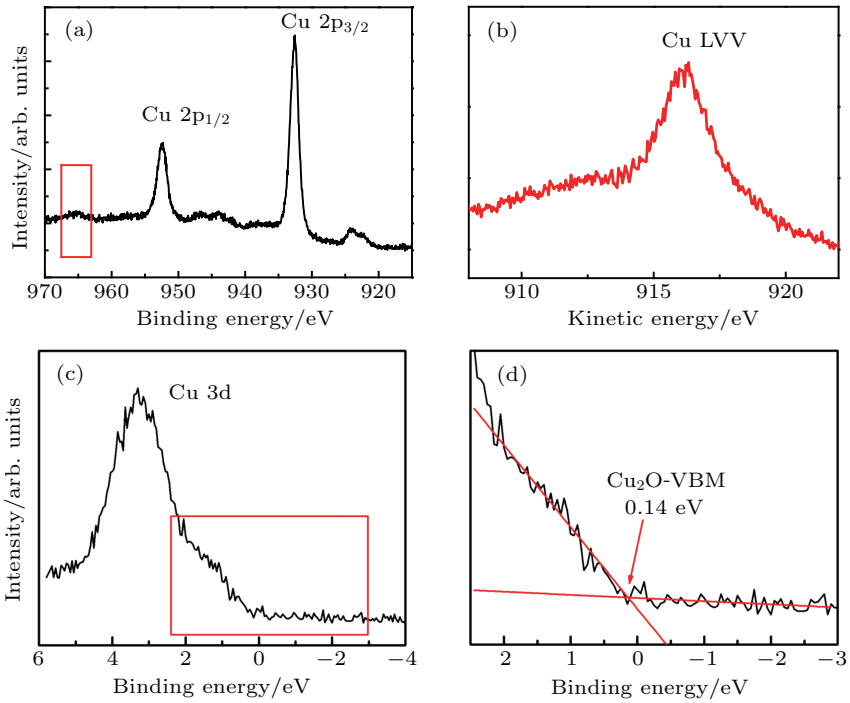


Fig. 4. (a) XPS survey scan of Cu $2p_{1/2}$ and Cu $2p_{3/2}$ CL spectrum, (b) XAES of Cu LVV, (c) valence band spectrum, and (d) VBM determination of 100 nm-Cu_2O/100 nm-ZnO/c-Al_2O_3.

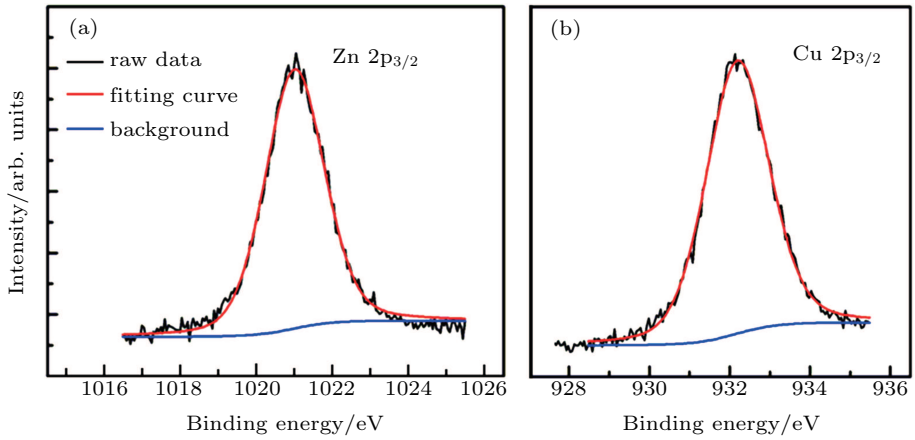


Fig. 5. (a) Zn $2p_{3/2}$ CL spectrum and (b) Cu $2p_{3/2}$ CL spectrum of 10 nm-Cu_2O/100 nm-ZnO/c-Al_2O_3.

Table 1. Peak positions of core level and VBM used to calculate VBO of p-Cu_2O/n-ZnO heterojunction.

Sample	Region	Binding energy
n-ZnO	Zn $2p_{3/2}$	1021.35
	VBM	2.44
p-Cu_2O	Cu $2p_{3/2}$	932.21
	VBM	0.14
p-Cu_2O/n-ZnO	Zn $2p_{3/2}$	1021.00
	Cu $2p_{3/2}$	932.19

For clarity, all of the peak energy values of CL and VBM achieved from 100 nm-ZnO/c-Al_2O_3, 100 nm-Cu_2O/100 nm-ZnO/c-Al_2O_3, and 10 nm-Cu_2O/100 nm-ZnO/c-Al_2O_3 are summarized in Table 1. By inserting the relevant peak parameters into Eq. (1), the VBO of the Cu_2O/ZnO heterojunction is calculated to be 1.97 eV. Given the optical band gap of 3.37 eV for ZnO and 2.17 eV for Cu_2O, we obtain a type-II staggered band alignment with a CBO of 0.77 eV as shown

schematically in Fig. 6. Different values for the CBO in the Cu_2O/ZnO heterojunction have been reported.[33–35] The main improvement is due to the reduction of the CBO, which leads to an increase in the open circuit voltage.[7] In our study, a CBO of 0.77 eV is achieved, which is smaller than these earlier results. As is well known, the open circuit voltage (V_{oc}) is determined by the difference in electrochemical potential between the hole and electron. In the energy band alignment of the pCu_2O-nZnO heterojunction, the thermodynamic limit for V_{oc} is approximately deduced by subtracting the CBM of ZnO from the VBM of Cu_2O. In our study, the thermodynamic limit for V_{oc} is calculated to be 1.4 eV, much higher than the experimental result at a low range of 0.2 V–0.8 V,[36–38] which is also of benefit to the efficiency enhancement of Cu_2O/ZnO solar cells.

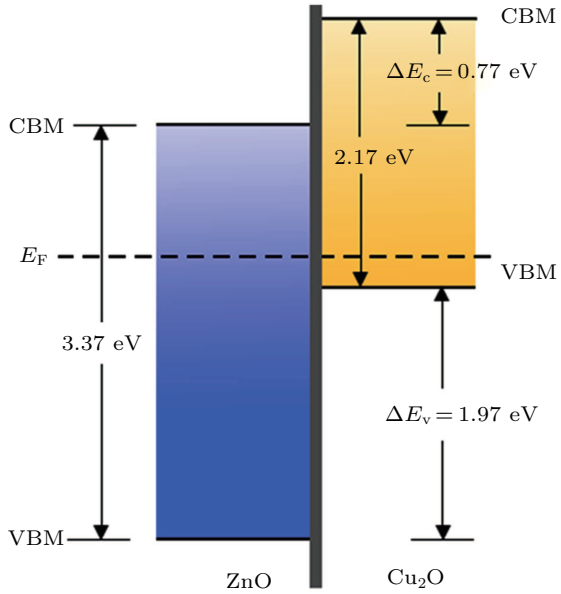


Fig. 6. Band alignment for the heterostructure p-Cu_2O/n-ZnO.

4. Conclusions

In this work, we successfully fabricated a high-quality p-Cu_2O/n-ZnO heterojunction. By *in situ* XPS, the VBO of the Cu_2O/ZnO heterojunction is determined to be 1.97 eV. Given the band gap difference of 1.20 eV between two materials, this translates into a staggered interface band alignment with a CBO of 0.77 eV. The determination of the band alignment is beneficial to understanding the electronic transport mechanism and improving the photoelectrical properties of Cu_2O/ZnO solar cells.

References

[1] Minami T, Nishi Y, Miyata T and Nomoto J 2011 *Appl. Phys. Express* **4** 062301
[2] Wick R and Tilley S D 2015 *J. Phys. Chem. C* **119** 26243
[3] Raebiger H, Lany S and Zunger A 2007 *Phys. Rev. B: Condens. Matter* **76** 045209
[4] Lany S and Zunger A 2007 *Phys. Rev. Lett.* **98** 045501
[5] Minami T, Miyata T and Nishi Y 2014 *Thin Solid Films* **559** 105
[6] Lofeski J J 1956 *J. Appl. Phys.* **27** 777
[7] Minami T, Nishi Y and Miyata T 2016 *Appl. Phys. Express* **9** 052301
[8] Sebastian S, Hellmann J C, Tilley S D, Graetzel M, Morasch J, Deuermeier J, Jaegermann W and Klein A 2016 *ACS Appl. Mater. Interfaces* **8** 21824
[9] Wilson S S, Tolstova Y, Scanlon D O, Watson G W, Atwater H A and Bosco J P 2014 *Energy Environ. Sci.* **7** 3606
[10] Lin P, Chen X, Yan X, Zhang Z, Yuan H, Li P, Zhao Y and Zhang Y 2014 *Nano Res.* **7** 860
[11] Kang Z, Yan X, Wang Y, Bai Z, Liu Y, Zhang Z, Lin P, Zhang X, Yuan H, Zhang X and Zhang Y 2015 *Sci. Rep.* **5** 7882
[12] Xu C, Cao L, Su G, Liu W, Liu H, Yu Y and Qu X 2010 *J. Hazard. Mater.* **176** 807
[13] Ievskaya Y, Hoye R L Z, Sadhanala A, Musselman K and MacManus-Driscoll J L 2015 *Sol. Energy Mater. Sol. Cells* **135** 43
[14] Ishizuka S, Suzuki K, Okatomo Y, Yanagita M, Sakurai T, Akimoto K, Fujiwara N, Kobayashi H, Matsubara K and Niki S 2004 *Phys. Status Solidi* **4** 1067
[15] Mittiga A, Salza E, Sarto F, Tucci M and Vasanthi R 2006 *Appl. Phys. Lett.* **88** 163502
[16] Tanaka H, Shimakawa T, Miyata T, Sato H and Minami T 2005 *Appl. Surf. Sci.* **244** 568
[17] Minami T, Miyata T, Ihara K, Minamino Y and Tsukada S 2006 *Thin Solid Films* **494** 47
[18] Dong C J, Yu W X, Xu M, Cao J J, Chen C, Yu W W and Wang Y D 2011 *J. Appl. Phys.* **110** 073712
[19] Zhang P F, Liu X L, Zhang R Q, Fan H B, Yang A L, Wei H Y, Jin P, Yang S Y, Zhu Q S and Wang Z G 2008 *Appl. Phys. Lett.* **92** 012104
[20] Cho H, Douglas E A, Gila B P, Craciun V, Lambers E S, Ren F and Pearton S J 2012 *Appl. Phys. Lett.* **100** 012105
[21] Fan H B, Sun G S, Yang S Y, Zhang P F, Zhang R Q, Wei H Y, Jiao C M, Liu X L, Chen Y H, Zhu Q S and Wang Z G 2008 *Appl. Phys. Lett.* **92** 192107
[22] Kraut E, Grant R, Waldrop J and Kowalczyk S 1980 *Phys. Rev. Lett.* **44** 1620
[23] Alay J L, Hirose M 1997 *J. Appl. Phys.* **81** 1606
[24] Perego M and Seguini G 2011 *J. Appl. Phys.* **110** 053711
[25] Su S C, Lu Y M, Zhang Z Z, Shan C X, Li B H, Shen D Z, Yao B, Zhang J Y, Zhao D X and Fan X W 2008 *Appl. Phys. Lett.* **93** 082108
[26] You J B, Zhang X W, Zhang S G, Tan H R, Ying J, Yin Z G, Zhu Q S and Chu P K 2010 *J. Appl. Phys.* **107** 083701
[27] Wang X J, Wang X L, Xiao H L, Wang C M, Feng C, Deng Q W, Qu S Q, Zhang J W, Hou X, Cai S J and Feng Z H 2013 *Chin. Phys. Lett.* **30** 057101
[28] Lu Y, Le Breton J C, Turban P, Lépine B, Schieffer P and Jézéquel G 2006 *Appl. Phys. Lett.* **88** 042108
[29] Li Y F, Yao B, Lu Y M, Li B H, Gai Y Q, Cong C X, Zhang Z Z, Zhao D X, Zhang J Y, Shen D Z and Fan X W 2008 *Appl. Phys. Lett.* **92** 192116
[30] Poulston S, Parlett P M, Stone P and Bowker M 1996 *Surf. Interface Anal.* **24** 811
[31] Barman S R and Sarma D D 1992 *J. Phys. Condens. Matter* **4** 7607
[32] Tobin J P, Hirschwald W and Cunningham J 1983 *Appl. Surf. Sci.* **16** 441
[33] Ichimura M, Song Y 2011 *Jpn. J. Appl. Phys.* **50** 051002
[34] Kramm B, Laufer A, Reppin D, Kronenberger A, Hering P, Polity A and Meyer B K 2012 *Appl. Phys. Lett.* **100** 094102
[35] Yang M, Zhu L, Li Y, Cao L and Guo Y 2013 *J. Alloys Compd.* **578** 143
[36] Wong L M, Chiam S Y, Huang J Q, Wang S J, Pan J S and Chim W K 2010 *J. Appl. Phys.* **108** 033702
[37] Chen S J, Lin L M, Liu J Y, Lv P W, Wu X P, Zheng W F, Qu Y and Lai F C 2015 *J. Alloys Compd.* **644** 378
[38] Nishi Y, Miyata T and Minami T 2013 *Thin Solid Films* **528** 72